ELSEVIER

Journal of Hydrology 237 (2000) 100–112

Journal of Hydrology

www.elsevier.com/locate/jhydrol

The use of temperature and the isotopes of O, H, C, and noble gases to determine the pattern and spatial extent of groundwater flow

E.R. James[a], M. Manga[a,*], T.P. Rose[b], G.B. Hudson[b]

[a]*Department of Geological Sciences, University of Oregon, Eugene, OR 97403, USA*
[b]*Analytical and Nuclear Chemistry Division, Lawrence Livermore National Laboratory, Livermore, CA 94550, USA*

Received 20 December 1999; revised 5 June 2000; accepted 14 July 2000

Abstract

Isotopic tracer and temperature measurements at large volume cold springs in the central Oregon Cascades are used to understand the pattern of groundwater flow. Standard oxygen and hydrogen isotope interpretations are used to determine the mean recharge elevation for springs. Carbon and helium isotopes are used to measure the component of dissolved magmatic gas in the spring waters. Inferences from isotopic measurements are compared with temperature measurements made at the springs to determine whether groundwater circulates to shallow or deep depths in the subsurface. Integrating the measurements of tracers derived at the surface, tracers derived from the subsurface, and temperature measurements can thus be used to derive a three dimensional picture of groundwater flow.

Keywords: Springs; Tracers; Helium; Carbon; Stable isotopes; Temperature

1. Introduction

Two commonly addressed questions in hydrogeologic investigations are

1. where does water come from (where is the source, or recharge area for groundwater)?
2. where does water go (what is the depth and lateral extent of the groundwater circulation)?

These questions refer to the spatial scale of groundwater flow, in which a groundwater flow system can be divided conceptually into "local" groundwater flow and "regional" groundwater flow (e.g. Tóth, 1962, 1963; Freeze and Witherspoon, 1967). Local flow is confined within a single basin enclosed by topographic high points, and circulates to relatively shallow depths in the subsurface. Regional flow circulates to greater depths and is not necessarily confined within a single hydrologic basin. A schematic illustration of different scales of groundwater flow is given in Fig. 1. For the remainder of this discussion, "scale" refers to both the lateral extent of groundwater flow (i.e. the distance between recharge and discharge area) and the depth of groundwater flow (i.e. deep or shallow). The most common approach to answering questions 1 and 2 is to apply numerical groundwater flow models that are constrained by well data, including head measurements, hydraulic conductivity measurements, and tracer data, in addition to geologic information (e.g. Anderson and Woessner, 1992).

In some locations, such as the central Oregon

* Corresponding author. Tel.: +1-541-346-5574; fax: +1-541-346-4692.
E-mail address: manga@newberry.uoregon.edu (M. Manga).

0022-1694/00/$ - see front matter
PII: S0022-1694(00)00303-6

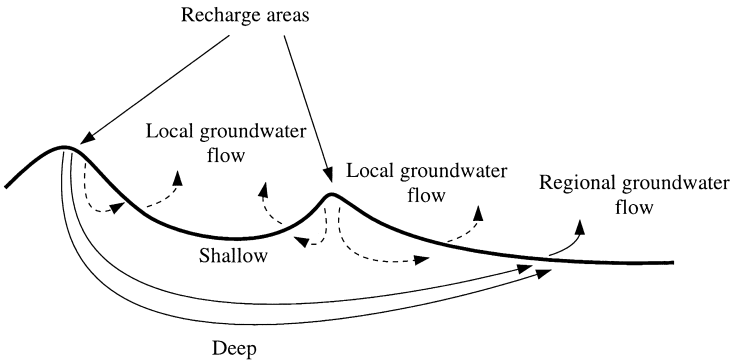

Fig. 1. A schematic illustration of the different scales of groundwater flow. Dashed arrows represent local flow and solid arrows represent regional flow.

Cascades studied here, there are few wells and boreholes to constrain these numerical models. However, by using a combination of tracer data and temperature measurements at springs, it is possible to understand the spatial scale of groundwater flow. Oxygen and hydrogen isotopes are commonly used to determine the average elevation of recharge for a particular mass of groundwater (e.g. Christodoulou et al., 1993; Scholl et al., 1996; Williams and Rodoni, 1997). In volcanic regions such as the Oregon Cascades, carbon and helium isotopes have been used to demonstrate the presence of magmatic gases dissolved in groundwater (Allard et al., 1991, 1997; Rose and Davisson, 1996; Reid et al., 1998; Sorey et al., 1998; James et al., 1999). Deeply circulating groundwater may preferentially dissolve magmatic gases and advectively transport them to springs, whereas groundwater that circulates to shallow depths might not have the opportunity to dissolve magmatic gases along the flowpath.

Circulating groundwater will acquire geothermal heat along its flowpath. In the Oregon Cascades, the high permeability of near-surface rocks permits rapid infiltration of groundwater. Because groundwater advectively transports geothermal heat laterally from the recharge area to the discharge point, there is a near-zero, near-surface heat flux and temperature gradient in the recharge area (Ingebritsen et al., 1989). Despite the cold temperatures of springs in the central Oregon Cascades, a substantial amount of geothermal heat may be discharged at these points, particularly given the large volume of groundwater that emerges at some springs (Brott et al., 1981; Forster and Smith, 1989). Temperature measurements at springs are therefore one means of assessing the relative scale of groundwater flow because deeply circulating groundwater will acquire more geothermal heat than groundwater that circulates to shallow depths. Temperature measurements at springs thus provide an independent constraint on the depth of groundwater circulation.

The goal of the present study is to show how a variety of isotopic and temperature measurements can be integrated to answer the two questions posed at the beginning of this section for the special case of large-volume spring systems. In this study, we analyze the hydrogen and oxygen isotope content of springs to determine the mean recharge elevation for spring discharge. We also analyze the dissolved ^{14}C and helium isotope content to determine whether magmatic volatiles are present in the groundwater. Each of these tracer measurement and interpretation techniques is well established and commonly used in hydrologic studies (e.g. Nativ et al., 1999). Our new contribution is to integrate the use of tracers derived from both the surface and the subsurface with temperature measurements to provide a conceptual model of groundwater flow for this region.

2. Geologic and hydrologic setting

The Cascade arc formed as a result of subduction-related volcanism over the last 40 m.y.. The “High Cascades” physiographic subprovince is composed of $\leq$7 Ma tholeiitic and calc-alkaline basaltic lava

flows and tephras and basaltic to rhyolitic intrusions (Walker and MacLeod, 1991). The most recent volcanic activity in central Oregon occurred at Belknap Crater 1500 ybp and South Sister 1900 ybp (Wood and Kienle, 1990). In the central Oregon Cascades, from Mt. Jefferson to south of Crater Lake, the crest of the Cascade range is composed of overlapping basalt and basaltic andesite shield volcanoes (Ingebritsen et al., 1994). The largest peaks in the central Oregon Cascades are shown in Fig. 2. The permeable rocks that make up the High Cascades serve as the primary groundwater recharge area for aquifers located to the east and west.

The High Cascades are responsible for the dramatic rainshadow effect to the east of the range (see inset of Fig. 2). Precipitation in the High Cascades of Oregon, mainly in the form of snowfall, can be as high as 3 m rain-equivalent per year, but in the study area, located to the east of the crest, mean annual precipitation can be as low as 0.25 m. East of the crest, where aquifers are typically composed of permeable Quaternary volcanic rocks, large volume springs discharge cold water near contacts between the permeable volcanic rocks and less permeable sedimentary rocks, or along structural boundaries. These cold springs are predominantly mixed cation bicarbonate waters, with low concentrations of total dissolved solids (Caldwell, 1998). Spring-fed streams in this region also have nearly constant discharge throughout the year (Whiting and Stamm, 1995).

3. Methods

Water samples were collected from both small and large volume springs at various times during the period 1995–1999 (Fig. 2). Snow cores were also collected during winter and early spring 1998 in order to determine the local distribution of oxygen and hydrogen isotopes in precipitation. Some of the sampled springs have large volume discharges (0.7–7 m^3/s) and form the headwaters of major streams in the region. Oxygen and hydrogen isotopic analyses were conducted for most water samples. Large volume springs were also analyzed for their dissolved inorganic carbon isotope content ($\delta^{13}C$, ^{14}C) and select large volume springs were analyzed for helium isotopes.

A total of 76 snow samples were collected from the central Oregon Cascades (Fig. 2). All snow cores were taken from areas where the snow pack melts completely in spring or early summer. Snow cores were placed in plastic bags and allowed to melt completely. The melted snow was then transferred to glass bottles with airtight caps to prevent exchange with atmospheric water vapor. Forty-eight water samples were collected from cold springs (temperatures between 2 and 12°C) to the east of the Cascade crest (Fig. 2) and stored in a similar manner. Samples were prepared for isotopic analysis using the water–CO_2 equilibration method for oxygen (Epstein and Mayeda, 1953) and the zinc-reduction method for deuterium (Coleman et al., 1982). Isotope analyses were performed on an isotope ratio mass-spectrometer. Results are reported in the conventional δ-notation as per mil deviations from the SMOW reference standard. $\delta^{18}O$ at springs varied by less than 0.1‰ over the period of study. All data are reported in James (1999); select data are shown in Table 1.

Waters were collected for carbon isotope analysis from eight large volume cold springs in the central Oregon Cascades (data in Table 1; see Fig. 7 for locations of specific springs discussed in this text). Samples were treated in the field with $HgCl_2$ to prevent biological fractionation of isotopes. Samples were stored in glass bottles with airtight seals to prevent exchange with atmospheric CO_2. DIC was extracted from the water using a dynamic vacuum-line acid stripping technique that uses H_3PO_4 to acidify the water. The resulting CO_2 gas was liberated from the sample using a nitrogen carrier gas, and trapped cryogenically. CO_2 splits were made for $\delta^{13}C$ and ^{14}C analysis. Samples intended for ^{14}C analysis were reduced to graphite at 570°C by using hydrogen gas and a cobalt metal catalyst. ^{14}C measurements were made on the accelerator mass spectrometer at Lawrence Livermore National Laboratory. $\delta^{13}C$ analyses were made with an isotope ratio mass spectrometer. $\delta^{13}C$ analyses are reported as per mil deviations from the PeeDee Belemnite standard; ^{14}C values are reported as percent modern carbon (pmc). An additional sample discussed in this paper is from Caldwell (1998). Data are reported in Table 1.

Samples were collected from four springs for helium isotope analysis. Water was pumped through

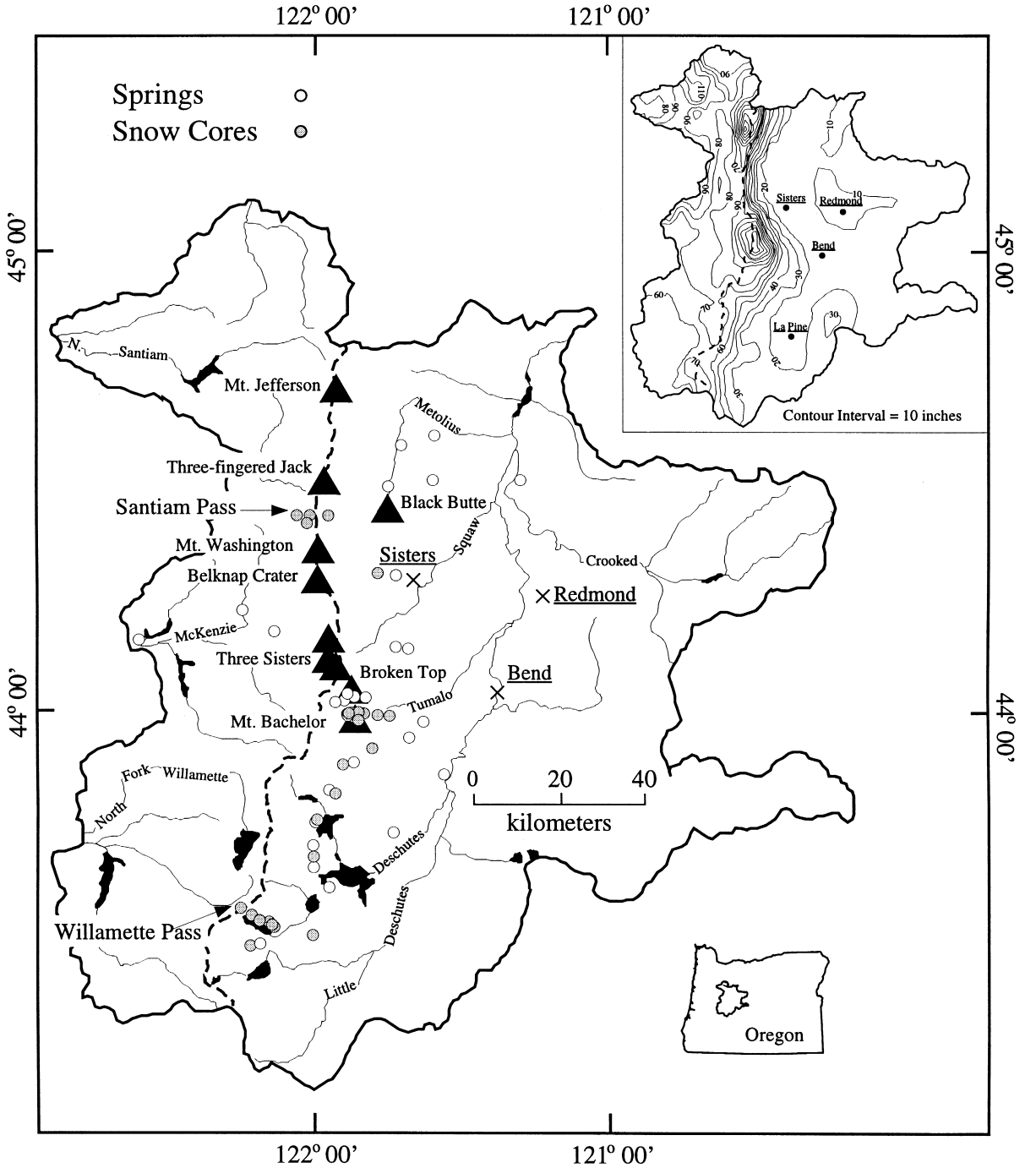

Fig. 2. Sampling locations. The north–south trending dashed curve is the approximate crest of the central Oregon high Cascades. Inset shows mean annual precipitation for the study area. Precipitation map is from the State Service Center for Geographic Information Systems.

Table 1
Isotope and temperature data for large springs

Spring	Elev. (m)	Temp. (°C)	Disch. (m^3/s)[a]	$\delta^{18}O$ (‰)	$\delta^{13}C$ (‰)	^{14}C (pmc)	^{4}He (atoms/g)	^{3}He (atoms/g)	Ar (atoms/g)	^{3}H (TU)[b]	$^{3}He/^{3}H$ Age (yrs)
Brown's	1332	3.8	1.1	−13.9	−16.4	115.3	1.18×10^{12}	1.63×10^{6}	1.13×10^{16}	6.9	0.7
Cultus	1356	3.4	1.8	−14.1	−15.8	113.9	1.15×10^{12}	1.65×10^{6}	1.04×10^{16}	9.0	2.5
Fall	1286	6.1	4.2	−14.2	−11.8	110.9	–	–	–	–	–
Lower Opal[c]	597	12.0	6.8	−15.3	−12.7	60.0	–	–	–	0.8	–
Metolius	920	8.2	3.1	−14.7	−11.5	61.3	1.71×10^{12}	4.89×10^{6}	9.56×10^{15}	4.0	47.4
N. Davis	1323	3.4	–	−14.1	−15.8	114.0	–	–	–	–	–
Quinn	1354	3.4	0.7	−13.7	−16.5	112.3	1.16×10^{12}	1.66×10^{6}	1.05×10^{16}	8.1[d]	2.1
Snow	1378	5.5	0.8	−14.1	−12.9	111.1	–	–	–	–	–
Spring	1268	8.0	3.5	−14.6	−11.5	67.5	–	–	–	–	–

[a] USGS gauging-station measurements, except for Metolius, from Meinzer (1927).
[b] Error for tritium analysis: Brown's, Cultus, Metolius error is ±0.5 (2-sigma), Quinn error is ±2.7 (1-sigma).
[c] Data from Caldwell (1998).
[d] Data from Manga (1997).

submerged copper tubes attached to Tygon tubing until no air bubbles were visible. The copper tubes were then clamped shut. Separate 500 ml samples were collected for tritium analysis. Tritium analyses were made using the ^{3}He accumulation method (Surano et al., 1992). Data are reported in Table 1.

Temperature, pH, alkalinity, and conductivity were also measured in the field. Sampling locations are shown in Fig. 2. Temperature measurements were made at springs at the time of collection with a calibrated thermometer with a precision of 0.1°C. Temperature measurements at individual springs varied by less than 0.3°C throughout the year.

4. Results and discussion

An analysis of snow core data indicates that in the central Oregon Cascades there is a decrease in δ^{18}O of 0.18‰ per 100 m rise in elevation, which is similar to the −0.2‰ shift per 100 m rise in elevation reported by Dansgaard (1964) for temperate climates. The slopes of these relationships are similar to, but also slightly less than slopes found for other locations in the Pacific Northwest. Clark et al. (1982) found a decrease in δ^{18}O of 0.25‰ per 100 m rise in elevation for the coast mountains of British Columbia and Rose et al. (1996) found a decrease of 0.23‰ per 100 m rise in elevation in the southern Cascades.

The negative relationship between δ^{18}O and elevation differs from the positive relationship between δ^{18}O of small springs to the east of the crest and elevation reported in Ingebritsen et al. (1994). This difference can be accounted for by noting that a spring may discharge water that is recharged at a higher elevation than the springs (as shown later in Fig. 4). Indeed, our small spring δ^{18}O data (James, 1999) do show a wide degree of scatter like the Ingebritsen et al. (1994) data and perhaps also a slightly positive correlation with elevation (Fig. 6 in Ingebritsen et al., 1994). The large springs studied here lie on a meteoric water line similar to that of the snow cores and the global meteoric water line (Fig. 3). In contrast, many of the small springs considered by Ingebritsen et al. (1994) fall well below the global meteoric water line suggesting that evaporation may have affected the water discharged at the small springs (see also Fig. 2 in Manga, 1997). We also note that there is substantial variability in the isotopic composition of snow from this region. This scatter results from the variation in isotopic composition of snow from different precipitation events and kinetic processes that occur as the snowpack ages on the ground surface, including sublimation and diffusion of water vapor through the snow (Moser and Stichler, 1980; Friedman et al., 1991).

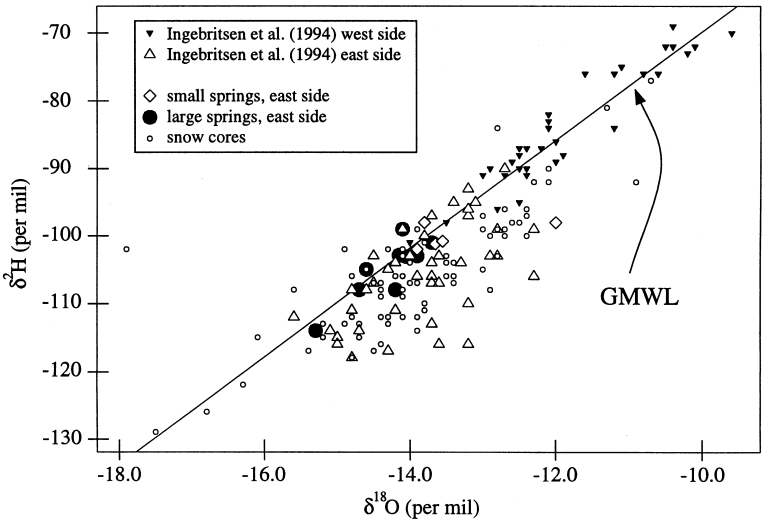

Fig. 3. Relationship between δ^{18}O and δ^{2}H for both springs and snow samples. GMWL is the global meteoric water line given by $\delta^{2}H = 8\delta^{18}O + 10$.

Scatter also results from the fact that samples are from the east side of the Cascade crest where precipitation rates are relatively low in comparison to the west side of the crest.

Given the relationship between $\delta^{18}O$ in precipitation and elevation, we determine an approximate mean recharge elevation for the large springs included in this study (Fig. 4). An inherent assumption in this type of analysis is that the spring water is young enough to be comparable to modern precipitation. This assumption appears to be reasonable in light of $^{3}He/^{3}H$ ages (discussed later) that indicate mean groundwater residence times for these springs on the order of tens of years or less. The Quinn River, Cultus River, and Brown's Creek Springs are all recharged near the Cascade crest, approximately 10 km west of these springs.

Other large springs have inferred recharge elevations that suggest more remote recharge areas. The Metolius River for example, is located at a relatively low elevation (920 m), yet the inferred mean recharge elevation (~2200 m) is consistent with recharge along the Cascade crest, over 30 km from the spring. Lower Opal Spring (597 m) is also recharged at a high elevation (~2500 m), although the crest of the Cascades is 50 km from the spring. From oxygen and hydrogen isotope data, it is reasonable to infer that both the Metolius River and Lower Opal Springs discharge groundwater derived from areas outside the immediate drainage basin. Furthermore, precipitation near Lower Opal Springs is less than 0.25 m/yr, which is not volumetrically sufficient to account for the large spring discharge.

By measuring the carbon isotope content of dissolved inorganic carbon (DIC) in large cold springs, it is possible to demonstrate the presence of diffuse emissions of magmatically derived gases dissolved in the groundwater (Allard et al., 1991; Rose and Davisson, 1996; Rose et al., 1996; Sorey et al., 1998). Three spring waters have a component of dissolved magmatic carbon: the Metolius River, Spring Creek (James et al., 1999), and Lower Opal Spring (Caldwell, 1998). Carbon isotope data are shown in Fig. 5. Minnehaha soda spring ($\delta^{13}C = -7.3‰$; $^{14}C = 0.2$ pmc) located in southern Oregon, represents the inferred magmatic DIC endmember (Rose and Davisson, 1996). Low ^{14}C concentrations in this region are unlikely to result from carbonate dissolution or groundwater aging (James et al., 1999). It is interesting to note that most of the large, cold springs have no component of dissolved magmatic gas. This suggests that either the diffuse flux of magmatic gas in this region is unevenly distributed or that groundwater encounters

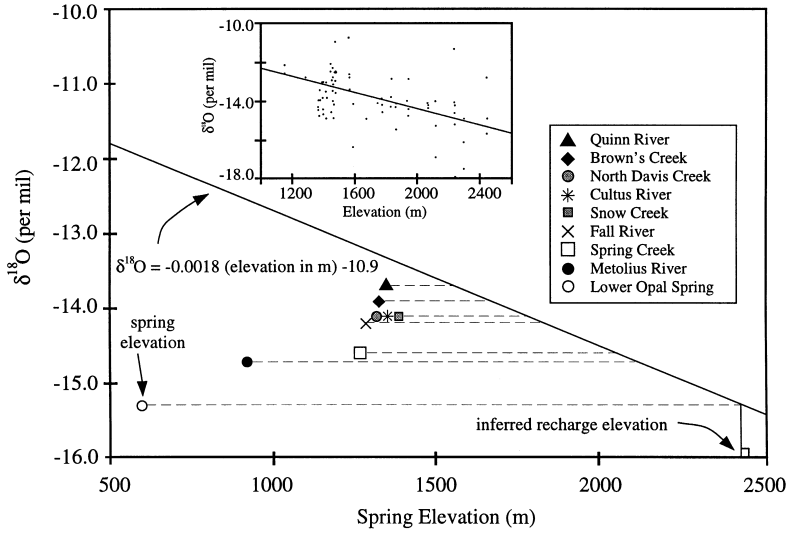

Fig. 4. Determination of recharge elevations from the relationship between $\delta^{18}O$ in snow and elevation. Approximate recharge elevations can be determined by extrapolating from the spring isotopic composition to the regression line, then dropping a perpendicular to the abscissa. Inset is the precipitation data used to constrain the regression line.

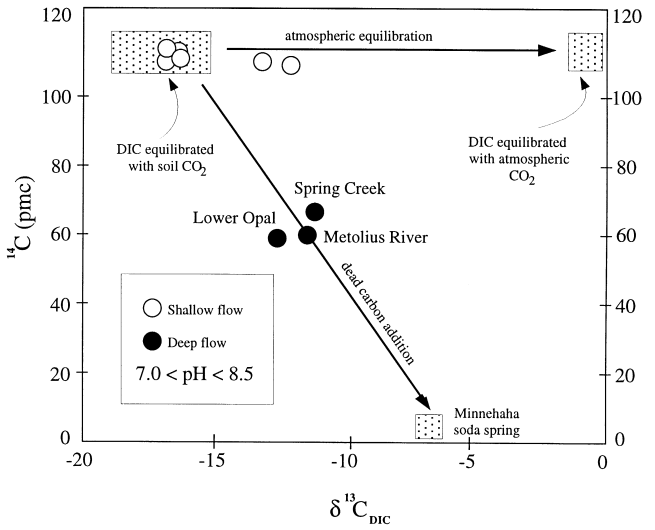

Fig. 5. Relationship between ^{14}C and $\delta^{13}C$ for large, cold springs. Stippled boxes represent the endmember isotopic compositions for water equilibrated with soil, atmospheric, and magmatic CO_2. The Oregon magmatic DIC endmember is represented by Minnehaha soda spring in southern Oregon (Rose and Davisson, 1996).

the magmatic volatiles only along deep flowpaths. The oxygen isotope data (Fig. 4) support the latter hypothesis in which the springs with dissolved magmatic carbon represent regional-scale flow.

Helium data were collected for Brown's Creek, Cultus River, Quinn River and the Metolius River. There are three reservoirs that contribute helium to groundwater — the atmosphere, mantle, and crust. The $^3He/^4He$ ratios in these reservoirs differ by up to three orders of magnitude, which makes contributions from each readily identifiable in fumarolic gases (Marty and Jambon, 1987). For groundwaters, identifying the contribution from each reservoir is more complicated, but still possible (e.g. Cook et al., 1996; Bethke et al., 1999). The $^3He/^4He$ ratio in the atmosphere is 1.386×10^{-6} (Marty and Le Cloarec, 1992). ^3He is also produced by the decay of ^3H from the atmosphere. Although ^3H is produced naturally in the atmosphere, concentrations increased by several orders of magnitude as a result of atmospheric thermonuclear weapons testing in the 1950s. The $^3He/^4He$ ratio of the mantle is on the order of 10^{-5} (Craig and Lupton, 1981) and crustal helium has a $^3He/^4He$ ratio of 10^{-8} as a result of radiogenic ^4He production from the decay of U- and Th-bearing minerals in the crust (Marty and Le Cloarec, 1992). Nucleogenic ^3He is also produced by the fission of ^6Li as a result of neutron production by the U/Th decay series. The measured concentrations of ^3He and ^4He in groundwater can thus be summarized as follows:

$$^3He_{total} = {}^3He_{atmosphere} + {}^3He_{tritogenic} + {}^3He_{nucleogenic} + {}^3He_{mantle} \quad (1)$$

and

$$^4He_{total} = {}^4He_{atmospheric} + {}^4He_{crustal} + {}^4He_{mantle}. \quad (2)$$

To determine the component of helium that is derived from a deep (e.g. mantle) source, it is necessary to correct for helium produced from other sources. We assume that the contribution of ^3He from nucleogenic sources is negligible because concentrations of ^6Li are likely to be low in the basaltic aquifer rocks.

Helium and tritium isotope data are shown in Table 1. The samples were corrected for excess air, i.e. air derived from the dissolution of small air bubbles caused by fluctuations in the water table (Heaton and Vogel, 1981), by using the measured value of Ar, and assuming high elevation recharge. Neither Brown's Creek, Quinn River, nor Cultus River contain observable non-atmospheric ^4He and all

non-atmospheric ^{3}He is assumed to be derived from ^{3}H decay. R/R_a, where R is the ^{3}He/^{4}He ratio of the sample and R_a is the same ratio in the atmosphere are 1.01, 1.04 and 1.05, respectively. The mixing of waters recharged at different times makes it difficult to determine a mean aquifer residence time, however, a ^{3}He/^{3}H "apparent age" can be calculated (Jenkins and Clarke, 1976). The ^{3}He/^{3}H ages for these springs are thus 0.7, 2.1 and 2.5 years, respectively, for Brown's Creek, Quinn River, and Cultus River. Given the young ages of the groundwater emerging at these springs, the mean aquifer thickness must be small. The mean residence time of water in an aquifer is equal to the volume of the water in the aquifer divided by the discharge. For the Cultus River, for example, assuming an aquifer area of 44 km^2 (Manga, 1997), which is reasonable based on topographic considerations and stable isotope data, a porosity of 10%, and a discharge of 1.8 m^3/s, the mean thickness of the aquifer would be about 30 m.

The Metolius River contains both non-atmospheric ^{3}He and excess ^{4}He. To determine the fraction of these excesses derived from mantle and crustal inputs, the amount of ^{3}He produced by tritium decay must be determined. Because mixing with water containing bomb-pulse ^{3}H will overwhelm any pre-1950s tritium input, it is difficult to derive an apparent ^{3}He/^{3}H age, $t_{apparent}$, greater than about 35 years (Aeschbach-Hertig et al., 1998; see also Manga (1999), Fig. 10). By assuming an apparent age of 35 years and by using the equation

$$t_{\text{apparent}}(\text{years}) = \frac{12.43}{\ln 2} \times \ln\left(1 + \frac{^3\text{He}_{\text{tritogenic}}}{^3\text{H}}\right), \quad (3)$$

where $^3\text{He}_{\text{tritogenic}}$ is the tritogenic helium concentration in the sample, and ^{3}H is the measured ^{3}H in the sample, the ^{3}H decay-corrected excess ^{3}He for the Metolius Headwaters is 2.0×10^6 atoms/g. If the groundwater is very young (i.e. just a few years), then no tritium correction is required and the $^3\text{He}_{\text{excess}}$ is 3.5×10^6 atoms/g.

The Metolius groundwater also has an excess of ^{4}He, which can be derived from either the crust, the mantle, or both. It is possible to estimate the fraction of ^{4}He from each source in a few different ways. Torgersen (1993) reports a range of ^{4}He fluxes from 0.5×10^{-18} to 13×10^{-18} mol cm^{-2} s^{-1}. If we assume that the entire flux of excess ^{4}He entering the Metolius drainage basin is discharged at the spring, we can calculate a flux of ^{4}He into the basin. The spring discharge is 3.1 m^3/s (Meinzer, 1927), the measured amount of excess ^{4}He (i.e. after correcting for air saturation) in the sample is 7.1×10^{11} atoms/g, and the drainage basin is approximately 400 km^2. Thus, 0.9×10^{-18} mol cm^{-2} s^{-1} of ^{4}He must be added to the Metolius drainage in order to account for the flux of excess ^{4}He observed at the spring. This value falls within the range reported by Torgersen (1993), but toward the low end of the range, which is consistent with the fact that bedrock in central Oregon is predominantly basaltic and has low U and Th concentrations relative to continental bedrock. Thus, the excess ^{4}He measured in the Metolius sample could all be derived from a crustal source with no added mantle component necessary to account for the measured ^{4}He concentration in the groundwater. However, because the spring contains excess (mantle-derived) ^{3}He, it is likely that some fraction of the ^{4}He in the Metolius groundwater is of mantle origin.

To estimate the fraction of ^{4}He in the Metolius waters that is derived from a mantle source, we can look at R/R_a for the sample. Typical magmatic gases in arc volcanoes have a R/R_a between 6 and 8, although both lower and higher values have been found (Welhan et al., 1988; Farley and Neroda, 1998). Austin, Bagby, and Breitenbush hot springs, located to the west of the Cascade crest in Oregon, have R/R_a values of 5.7, 1.2, and 6.5, respectively (Ingebritsen et al., 1994). If we assume a reasonable value of 8 for R/R_a for a gas from a mantle source, then the mantle contribution of ^{4}He ranges between 1.8 and 3.2×10^{11} atoms/g depending on the assumed apparent ^{3}H/^{3}He age. The corresponding crustal ^{4}He contribution is therefore between 3.9 and 5.3×10^{11} atoms/g, which implies a crustal ^{4}He flux of between 0.5×10^{-18} and 0.7×10^{-18} mol cm^{-2} s $-$ 1. From the carbon and helium (for the Metolius) isotope measurements, it is thus possible to conclude that the Metolius River, Spring Creek, and Lower Opal Springs have a component of dissolved magmatic gas and that the other large volume cold springs included in this analysis (Cultus, Quinn, Brown's, Snow Creek, Davis Creek, and Fall River) do not. This indicates that the source of magmatic gas is unevenly distributed throughout the

region, or that the pattern of groundwater flow in this region determines the distribution of dissolved magmatic gases so that shallow groundwater does not dissolve magmatic gases. We will proceed to show that the latter hypothesis can explain the carbon and helium isotope results.

Circulating groundwater advectively transports geothermal heat. Based on simple mass and energy balance arguments, it is possible to estimate the geothermal heat flow averaged over the drainage basin (Brott et al., 1981; Manga, 1998). We will use the Metolius River as an example. Based on hydrogen and oxygen isotope data, the recharge area for the Metolius was found to be along the Cascade crest, which suggests that a basin size, or recharge area, of approximately 400 km^2 is reasonable. We will assume that all geothermal heat is discharged at the spring and there is no surface conductive heat flow. This assumption is consistent with the near-zero, near-surface temperature gradient measured in the high Cascades (Ingebritsen et al., 1989) as a result of rapid and voluminous groundwater recharge. The background geothermal heat flow Q can be calculated from

$$Q = \rho C \Delta T \frac{\text{spring discharge}}{\text{recharge area}} \quad (4)$$

where ΔT is the expected geothermal warming, ρ the density of water, and C the heat capacity of water (Manga, 1998). Borehole temperature measurements at high elevations near the Cascade crest indicate that near surface groundwaters are near 3°C (Ingebritsen et al., 1994). The temperature of the Metolius discharge is measured to be 8.2°C. From Eq. (4), we thus obtain Q of approximately 160 mW/m^2 with the reasonable assumption that all the background heat flux is discharged at the spring. Background geothermal heat flow measurements for the central Oregon Cascades are estimated to be in the range of 110–130 mW/m^2 based on deep borehole temperature measurements (Blackwell et al., 1982; Ingebritsen et al., 1992). The high heat flow calculated with Eq. (4) might indicate that the Metolius drains a larger region than assumed, or that the mean spring discharge is lower than the assumed value (Meinzer, 1927).

By using the mean recharge elevations obtained from the oxygen isotope analysis, it is possible to show graphically the degree to which groundwater in the Oregon Cascades has been warmed geothermally. In Fig. 6, we show the relationship between mean annual surface temperature and elevation for eight Oregon climate stations located in or near the

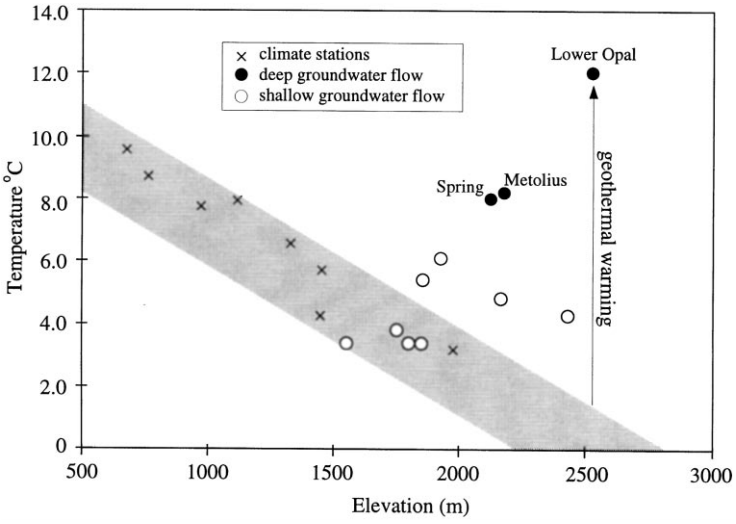

Fig. 6. Relationship between elevation and temperature for Oregon climate stations. The temperature of cold springs is shown as a function of the inferred mean recharge elevation determined from oxygen and deuterium isotope analysis. The Metolius River, Lower Opal Springs, and Spring Creek (closed circles) have higher measured temperatures that other large springs in this region and plot far from the mean annual surface temperature at the mean recharge elevation (shaded box).

study area. We also plot the calculated recharge elevation determined from the precipitation data and spring temperature for the springs included in Table 1. Metolius Headwaters, Lower Opal Springs and Spring Creek, have high measured temperatures of 8.2, 12.0 (Caldwell, 1998) and 8.3°C, respectively, and plot far from the mean annual surface temperatures found in the recharge area. In contrast, Quinn River, Cultus River, Brown's Creek, and Davis Creek have lower temperatures of 3.4, 3.4, 3.7, and 3.5°C, respectively, which are not significantly warmer than the mean annual surface temperature in the recharge area. The low temperatures of these latter springs are consistent with shallow circulation in the subsurface, but also require a deeper flow, not discharged at the springs, to remove geothermal heat.

The preceding analysis assumes that groundwater recharge enters the subsurface at temperatures near the mean annual surface temperature of the recharge area (Forster and Smith, 1989; Taniguchi, 1993). While this may be a good approximation, the actual recharge temperature is difficult to predict (Perez, 1997). This is because surface temperatures depend on slope orientation, slope angle, and microclimatic variations in addition to elevation (Blackwell et al., 1980). However, the fact that several springs,

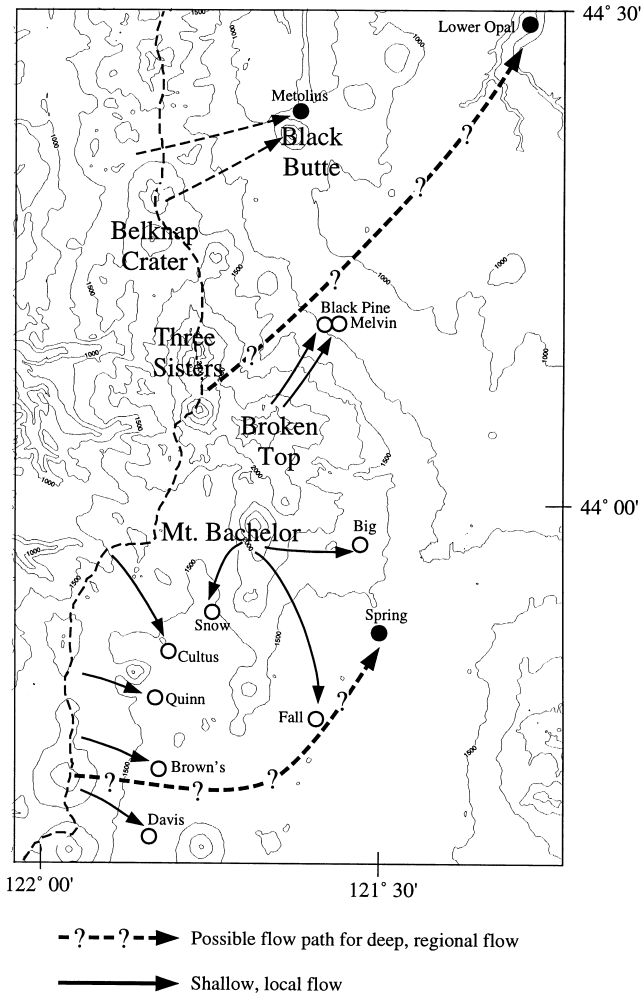

Fig. 7. Schematic illustration of groundwater flow in the central Oregon Cascades as determined from isotopic and temperature measurements. Dashed arrows represent regional groundwater flow and solid arrows represent local groundwater flow.

including the Metolius River, have temperatures significantly above the mean annual surface temperature for their respective recharge elevations implies that the groundwater acquires geothermal heat along the flow path.

5. Concluding remarks

In many volcanic terrains, including the central Oregon Cascades, surface waters are relatively scarce, and groundwater provides crucial water resources as well as habitat for fish and other wildlife (Whiting and Stamm, 1995). The population of Deschutes County, located in central Oregon, increased over 300% between 1970 and 1996 (Caldwell, 1998). The state of Oregon also closed surface water resources in this region to further appropriation, thus causing an increased demand for groundwater supplies. In this region, in particular, rapid population growth places heavy demands on available water supplies, which makes a general understanding of groundwater circulation patterns especially important.

By integrating isotopic and temperature measurements, we have determined that the Metolius River and Lower Opal Springs discharge groundwater derived from locations far (up to 50 km) from the springs themselves. Carbon and helium isotope analyses and temperature measurements indicate the groundwater discharged at these springs represents large-scale regional circulation. The remaining springs discharge locally derived groundwater that circulates to shallow depths in the subsurface. With these integrated measurements, we have been able to address the two questions posed in the introduction to this study and have developed a qualitative three-dimensional picture of groundwater flow in this region (Fig. 7). In the case of the Metolius River, there is not necessarily a shallow, local scale of flow above the deeper regional scale flow. In contrast, Lower Opal Springs and Spring River appear to be part of a multi-scale hydrologic system in which both regional and local scale flows are present.

Acknowledgements

The authors thank S. Ingebritsen and P. Fritz for thoughtful comments and helpful suggestions. Funding for this work was provided by the National Science Foundation, grant EAR 9701768.

References

Aeschbach-Hertig, W., Schlosser, P., Stute, M., Simpson, H.J., Ludin, A., Clark, J.F., 1998. A $^{3}H/^{3}He$ study of ground water flow in a fractured bedrock aquifer. Ground Water 34, 661–670.

Allard, P., Carbonnelle, J., Dajlevic, D., Le Bronec, J., Morel, P., Robe, M.C., Maurenas, J.M., Faivre-Pierret, R., Martin, D., Sabroux, J.C., Zettwoog, P., 1991. Eruptive and diffuse emissions of CO_2 from Mount Etna. Nature 351, 387–391.

Allard, P., Jean-Baptiste, P., D'Alessandro, W., Parello, F., Parisi, B., Flehoc, C., 1997. Mantle-derived helium and carbon in groundwaters and gases of Mount Etna, Italy. Earth Planet. Sci. Lett. 148, 501–516.

Anderson, M.P., Woessner, W.W., 1992. Applied Groundwater Modeling: Simulation of Flow and Advective Transport. Academic Press, San Diego, CA (381pp).

Bethke, C.M., Zhao, X., Torgersen, T., 1999. Groundwater flow and the ^{4}He distribution in the Great Artesian Basin of Australia. J. Geophys. Res. 104, 12999–13012.

Blackwell, D.D., Steele, J.L., Brott, C.A., 1980. The terrain effect on terrestrial heat flow. J. Geophys. Res. 85, 4757–4772.

Blackwell, D.D., Bowen, R.G., Hull, D.A., Riccio, J., Steele, J.L., 1982. Heat flow, arc volcanism, and subduction in northern Oregon. J. Geophys. Res. 87, 8735–8754.

Brott, C.A., Blackwell, D.D., Ziagos, J.P., 1981. Thermal and tectonic implications of heat flow in the eastern Snake River Plain, Idaho. J. Geophys. Res. 86, 11709–11734.

Caldwell, R.R., 1998. Chemical study of regional ground-water flow and ground-water/surface-water interaction in the upper Deschutes Basin, Oregon. US Geol. Surv. Water. Resour. Report 97-4233, 49pp.

Christodoulou, T., Leontiadis, I.L., Morfis, A., Payne, B.R., Tzimourtas, S., 1993. Isotope hydrology study of the Axios River plain in northern Greece. J. Hydrol. 146, 391–404.

Clark, I.D., Fritz, P., Michel, F.A., Souther, J.G., 1982. Isotope hydrogeology and geothermometry of the Mount Meager geothermal area. Can. J. Earth Sci. 19, 1454–1473.

Coleman, M.L., Shepherd, T.J., Durham, J.J., Rouse, J.E., Moore, G.R., 1982. Reduction of water with zinc for hydrogen isotope analysis. Anal. Chem. 54, 993–995.

Cook, P.G., Solomon, D.K., Sanford, W.E., Busenberg, E., Plummer, L.N., Poreda, R.J., 1996. Inferring shallow groundwater flow in saprolite and fractured rock using environmental tracers. Water Resour. Res. 32, 1501–1509.

Craig, H., Lupton, J., 1981. Helium-3 and mantle volatiles in the ocean and the oceanic crust. In: Emiliani, C. (Ed.). The Sea, vol. 7. Wiley, New York, NY.

Dansgaard, W., 1964. Stable isotopes in precipitation. Tellus 16, 436–463.

Epstein, S., Mayeda, T., 1953. Variation in ^{18}O content of waters from natural sources. Geochim. Cosmochim. Acta 4, 213–224.

Farley, K.A., Neroda, E., 1998. Noble gases in the Earth's mantle. Annu. Rev. Earth Planet. Sci. 26, 189–218.

Forster, C., Smith, L., 1989. The influence of groundwater flow on thermal regimes in mountainous terrain: a model study. J. Geophys. Res. 94, 9439–9451.

Freeze, R.A., Witherspoon, P.A., 1967. Theoretical analysis of regional groundwater flow. II. Effect of water-table configuration and subsurface permeability variation. Water Resour. Res. 3, 623–634.

Friedman, I., Benson, C., Gleason, J., 1991. Isotope changes during snow metamorphism. In: Taylor, H.P. (Ed.). Stable Isotope Geochemistry: A Tribute to Samuel Epstein, Geochemical Society, Special Publication No. 3 Geochemical Society, University Park, PA, pp. 211–221.

Heaton, T.H.E., Vogel, J.C., 1981. "Excess air" in groundwater. J. Hydrol. 50, 201–216.

Ingebritsen, S.E., Sherrod, D.R., Mariner, R.H., 1989. Heat flow and hydrothermal circulation in Cascade Range, north-central Oregon. Science 243, 1458–1462.

Ingebritsen, S.E., Sherrod, D.R., Mariner, R.H., 1992. Rates and patterns of groundwater flow in the Cascade Range volcanic arc, and the effect on subsurface temperatures. J. Geophys. Res. 97, 4599–4627.

Ingebritsen, S.E., Mariner, R.H., Sherrod, D.R., 1994. Hydrothermal systems of the Cascade Range, north-central Oregon. US Geol. Surv. Prof. Pap., 1044-L, 86pp.

James, E.R., 1999. Isotope tracers and regional-scale groundwater flow: application to the Oregon Cascades. Master's Thesis, University of Oregon, 150pp.

James, E.R., Manga, M., Rose, T.P., 1999. CO_2 degassing in the Oregon Cascades. Geology 27, 823–826.

Jenkins, W.J., Clarke, W.B., 1976. The distribution of ^{3}He in the western Atlantic Ocean. Deep-Sea Res. 23, 481–494.

Manga, M., 1997. A model for discharge in spring-dominated streams and implications for the transmissivity and recharge of quaternary volcanics in the Oregon Cascades. Water Resour. Res. 33, 1813–1822.

Manga, M., 1998. Advective heat transport by low-temperature discharge in the Oregon Cascades. Geology 26, 799–802.

Manga, M., 1999. On the timescales characterizing groundwater discharge at springs. J. Hydrol. 219, 56–69.

Marty, B., Jambon, A., 1987. C/^{3}He in volatile fluxes from the solid Earth: implications for carbon geodynamics. Earth Planet. Sci. Lett. 83, 16–26.

Marty, B., Le Cloarec, M.-F., 1992. Helium-3 and CO_2 fluxes from subaerial volcanoes estimated from polonium-210 emissions. J. Volcan. Geotherm. Res. 53, 67–72.

Meinzer, O.E., 1927. Large springs in the United States. US Geol. Surv. Wat. Supp. Pap. 557.

Moser, H., Stichler, W., 1980. Environmental isotopes in ice and snow. In: Fritz, J., Fontes, Ch. (Eds.). Handbook of Environmental Isotope Geochemistry, vol. 1 (the terrestrial environment). Elsevier, Amsterdam.

Nativ, R., Günay, G., Hötzl, H., Reichert, B., Solomon, D.K., Tezcan, L., 1999. Separation of groundwater-flow components in a karstified aquifer using environmental tracers. Appl. Geochem. 14, 1001–1014.

Perez, E.S., 1997. Estimation of basin-wide recharge rates using spring flow, precipitation, and temperature data. Ground Water 35, 1058–1065.

Reid, J.B., Reynolds, J.L., Connolly, N.T., Getz, S.L., Polissar, P.J., Winship, L.J., Hainsworth, L.J., 1998. Carbon isotopes in aquatic plants, Long Valley caldera, California as records of past hydrothermal and magmatic activity. Geophys. Res. Lett. 25, 2853–2856.

Rose, T.P., Davisson, M.L., 1996. Radiocarbon in hydrologic systems containing dissolved magmatic carbon dioxide. Science 273, 1367–1370.

Rose, T.P., Davisson, M.L., Criss, R.E., 1996. Isotope hydrology of voluminous cold springs in fractured rock from an active volcanic region, northeastern California. J. Hydrol. 179, 207–236.

Scholl, M.A., Ingebritsen, S.E., Janik, C.J., Kauahikaua, J.P., 1996. Use of precipitation and groundwater isotopes to interpret regional hydrology on a tropical volcanic island: Kilauea Volcano area, Hawaii. Water Resour. Res. 32, 3525–3537.

Sorey, M.L., Evans, W.C., Kennedy, B.M., Farrar, C.D., Hainsworth, L.J., Hausback, B., 1998. Carbon dioxide and helium emissions from a reservoir of magmatic gas beneath Mammoth Mountain, California. J. Geophys. Res. 103, 15303–15323.

Surano, K.A., Hudson, G.B., Failor, R.A., Sims, J.M., Holland, R.C., Maclean, S.C., Garrison, J.C., 1992. Helium-3 mass spectrometry for low-level tritium analysis of environmental samples. J. Radioanal. Nuclear Chem. Art. 161, 443–453.

Taniguchi, M., 1993. Evaluation of vertical groundwater fluxes and thermal properties of aquifers based on transient temperature-depth profiles. Water Resour. Res. 29, 2021–2026.

Torgersen, T., 1993. Defining the role of magmatism in extensional tectonics: helium 3 fluxes in extensional basins. J. Geophys. Res. 98, 16257–16269.

Tóth, J.A., 1962. A theory of groundwater motion in small drainage basins in central Alberta, Canada. J. Geophys. Res. 67, 4375–4387.

Tóth, J.A., 1963. A theoretical analysis of groundwater flow in small drainage basins. J. Geophys. Res. 68, 4795–4812.

Walker, G.W., MacLeod, N.S., 1991. Geologic map of Oregon. United States Geol. Surv, Reston, VA.

Welhan, J.A., Poreda, R.J., Rison, W., Craig, H., 1988. Helium isotopes in geothermal and volcanic gases of the western United States. I. Regional variability and magmatic origin. J. Volcan. Geotherm. Res. 34, 185–199.

Whiting, P.J., Stamm, J., 1995. The hydrology and form of spring-dominated channels. Geomorphology 12, 233–240.

Williams, A.E., Rodoni, D.P., 1997. Regional isotope effects and application to hydrologic investigations in southwestern California. Water Resour. Res. 33, 1721–1729.

Wood, C.A., Kienle, J., 1990. Volcanoes of North America: United States and Canada. Cambridge University Press, Cambridge (354pp).